JPE 8-1-7

Implementation of Direct Torque Control Method using Matrix Converter Fed Induction Motor

Hong-Hee Lee†, Hoang M. Nguyen* and Tae-Won Chun*

†*School of Electrical Engineering, University of Ulsan, Ulsan, Korea

ABSTRACT

This paper develops a direct torque control method (DTC) using a matrix converter fed induction motor. The advantages of matrix converters are combined with the advantages of the DTC technique; under the constraint of the unity input power factor, the required voltage vectors are generated to implement the conventional DTC method of induction motor. The proposed DTC algorithm is applied to induction motors and the experimental results are given in steady-state and transient conditions, while the discussion about the trend of the DTC method using the MC is also carried out. Furthermore, the entire system of the matrix converter configuration using 7.5kW IGBT module is explained in detail.

Keywords: matrix converter, induction motor, direct torque control method

1. Introduction

In the past two decades, due to the need to increase the quality and the efficiency of power supply and usage, the three phase matrix converter has become a major modern energy converter and has emerged from the previously conventional energy conversion modules as one of the best substitutions [1], [2]. It fulfills all the requirements of the conventionally used rectifier/DC-link/ inverter structures. Some advantages of the matrix converter can be seen as follows: the use of a compact voltage source, providing sinusoidal voltage with varying amplitude and frequency besides the sinusoidal input current and unity input power factor at the power supply side. As shown in Figure 1, a matrix converter has a simple topology and a compact design due to the lack of DC-link capacitor for energy storage.

Since the Direct Torque Control (DTC) method has been proposed in the mid 1980's, the DTC method has become one of the higher performance control strategies for AC machines to provide a very fast torque and flux control[3]. There are no requirements for coordinate transformation, PWM generation and current regulators. The DTC method is widely known to produce a quick and fast response in AC drives by selecting the proper voltage space vector according to the switching status of the inverter, which is determined by the error signal of reference flux linkage and torque with their estimated values and the position of the estimated stator flux.

For such advanced reasons, the combination of the advantages of the matrix converter with those of the direct torque control method is effectively possible according to [4]. However, this research only focuses on some simulation results and the experimental results are not

Manuscript received Sep. 21, 2007; revised Nov. 26, 2007
† Corresponding Author: hhlee@ulsan.ac.kr
Tel: +82-52-259-2187, Fax: +82-52-259-2187, Univ. of Ulsan
* School of Electrical Eng., Univ. of Ulsan

sufficiently given. Moreover, some drawbacks still exist in the DTC method because the torque and the flux ripple always exceed their bandwidths. Thus, many researchers have paid much attention to solve these problems in the DTC methods [5], [6].

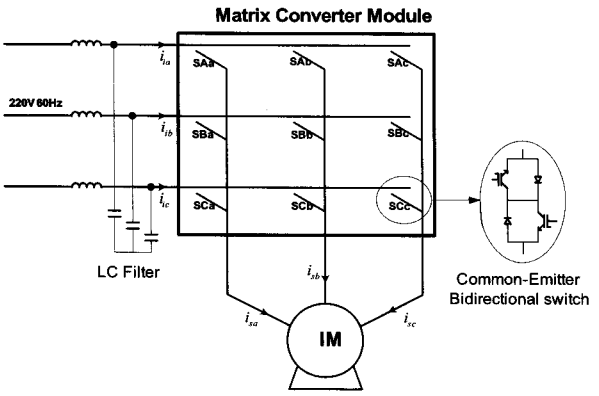

Fig. 1 Matrix converter schematic block diagram

In this paper, the DTC theory in the matrix converter module to control the induction motor is first explained and then the experimental results are provided in detail to verify the effectiveness of the DTC theory.

2. DTC Principles by Matrix Converter

2.1 Matrix Converter Theory

The three-phase matrix converter module includes nine bi-directional switches as shown in Figure 1. There are 27 switching configuration states, which mean 27 possible space vectors can be used to control IM and can be split respectively into 3 groups as shown in Table 1; in Group I, two output lines are connected to one of the other input lines; in Group II, all output lines are connected to a common input line; while in Group III, each output line is connected to a different input line. The corresponding output line-to-neutral voltage vector and input line current vector have fixed directions as represented in Figure 2. However, Group III is not useful. Only 18 non-zero space vectors in Group I (±1, ±2, ..., ±9) and 3 zero space vectors in Group II (0a, 0b, 0c) can be usually employed in the modern control techniques for the matrix converter (such as the Space Vector Modulation, DTC methods, etc.)

Table 1 Possible Switching Configurations of MC

Group	Vector	A B C	v_s	α_0	i_i	β_i
I	$+1_{MC}$	a b b	$2/3v_{ab}$	0	$2/\sqrt{3}i_{sa}$	$-\pi/6$
	-1_{MC}	b a a	$-2/3v_{ab}$	0	$-2/\sqrt{3}i_{sa}$	$-\pi/6$
	$+2_{MC}$	b c c	$2/3v_{bc}$	0	$2/\sqrt{3}i_{sa}$	$\pi/2$
	-2_{MC}	c b b	$-2/3v_{bc}$	0	$-2/\sqrt{3}i_{sa}$	$\pi/2$
	$+3_{MC}$	c a a	$2/3v_{ca}$	0	$2/\sqrt{3}i_{sa}$	$7\pi/6$
	-3_{MC}	a c c	$-2/3v_{ca}$	0	$-2/\sqrt{3}i_{sa}$	$7\pi/6$
	$+4_{MC}$	b a b	$2/3v_{ab}$	$2\pi/3$	$2/\sqrt{3}i_{sb}$	$-\pi/6$
	-4_{MC}	a b a	$-2/3v_{ab}$	$2\pi/3$	$-2/\sqrt{3}i_{sb}$	$-\pi/6$
	$+5_{MC}$	c b c	$2/3v_{bc}$	$2\pi/3$	$2/\sqrt{3}i_{sb}$	$\pi/2$
	-5_{MC}	b c b	$-2/3v_{bc}$	$2\pi/3$	$-2/\sqrt{3}i_{sb}$	$\pi/2$
	$+6_{MC}$	a c a	$2/3v_{ca}$	$2\pi/3$	$2/\sqrt{3}i_{sb}$	$7\pi/6$
	-6_{MC}	c a c	$-2/3v_{ca}$	$2\pi/3$	$-2/\sqrt{3}i_{sb}$	$7\pi/6$
	$+7_{MC}$	b b a	$2/3v_{ab}$	$4\pi/3$	$2/\sqrt{3}i_{sc}$	$-\pi/6$
	-7_{MC}	a a b	$-2/3v_{ab}$	$4\pi/3$	$-2/\sqrt{3}i_{sc}$	$-\pi/6$
	$+8_{MC}$	c c b	$2/3v_{bc}$	$4\pi/3$	$2/\sqrt{3}i_{sc}$	$\pi/2$
	-8_{MC}	b b c	$-2/3v_{bc}$	$4\pi/3$	$-2/\sqrt{3}i_{sc}$	$\pi/2$
	$+9_{MC}$	a a c	$2/3v_{ca}$	$4\pi/3$	$2/\sqrt{3}i_{sc}$	$7\pi/6$
	-9_{MC}	c c a	$-2/3v_{ca}$	$4\pi/3$	$2/\sqrt{3}i_{sc}$	$7\pi/6$
II	0_a	a a a	0	-	0	-
	0_b	b b b	0	-	0	-
	0_c	c c c	0	-	0	-
III	x	a b c	x	x	x	x
	x	a c b	x	x	x	x
	x	b c a	x	x	x	x
	x	b a c	x	x	x	x
	x	c a b	x	x	x	x
	x	c b a	x	x	x	x

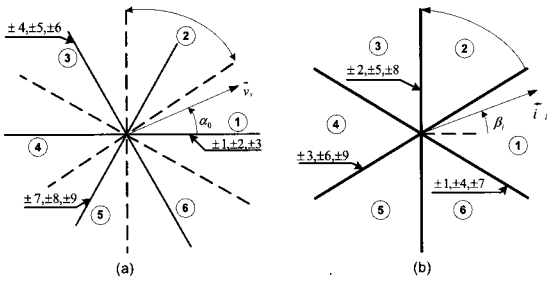

Fig. 2 (a) The output line-to-neutral voltage vectors
(b) The input line current vectors

2.2 DTC Principles Using VSI

In the conventional DTC principles, there are three main coefficients: a stator flux hysteresis, a torque hysteresis comparator and the position of the stator flux as

shown in Figure 3. In order to maintain the estimated stator flux and torque within their boundaries which are determined by the two hysteresis bandwidths as shown in figure 5a & 5b, at each sampling period, the torque and the stator flux are estimated and compared with the corresponding reference values before passing the hysteresis comparator. The position of the stator flux is detected, and the most suitable space vector among 8 space vectors generated by a VSI (6 non-zero space vector and two zero space vector in figure 4) is selected from the switching table given in Table 2 to compensate the load torque and the stator flux. Therefore, it is possible to implement the DTC schemes in having good and robust performances.

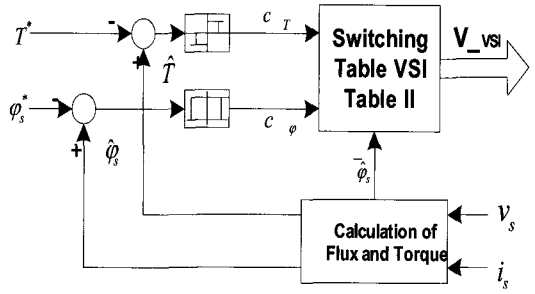

Fig. 3 The DTC diagram for VSI

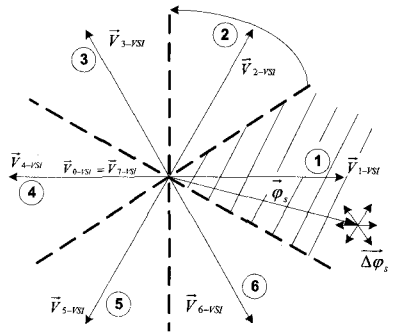

Fig. 4 VSI output line-to-neutral voltage vector and corresponding stator flux variation in period Δt

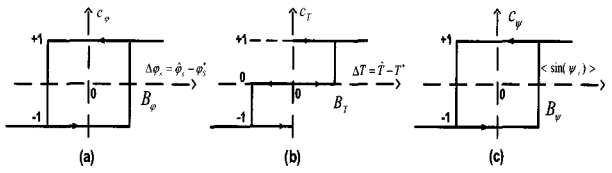

Fig. 5 (a) Flux hysteresis comparator
(b) Torque hysteresis comparator
(c) Hysteresis comparator of average sin(ψi)

Table 2 Basic DTC switching table using VSI

Sector of Flux→		1	2	3	4	5	6
$c_\varphi = 0$	c_T =-1	$V_{2\text{-vsi}}$	$V_{3\text{-vsi}}$	$V_{4\text{-vsi}}$	$V_{5\text{-vsi}}$	$V_{6\text{-vsi}}$	$V_{1\text{-vsi}}$
	$c_T = 0$	$V_{7\text{-vsi}}$	$V_{0\text{-vsi}}$	$V_{7\text{-vsi}}$	$V_{0\text{-vsi}}$	$V_{7\text{-vsi}}$	$V_{0\text{-vsi}}$
	$c_T = 1$	$V_{6\text{-vsi}}$	$V_{1\text{-vsi}}$	$V_{2\text{-vsi}}$	$V_{3\text{-vsi}}$	$V_{4\text{-vsi}}$	$V_{5\text{-vsi}}$
c_φ=+1	c_T =-1	$V_{3\text{-vsi}}$	$V_{4\text{-vsi}}$	$V_{5\text{-vsi}}$	$V_{6\text{-vsi}}$	$V_{1\text{-vsi}}$	$V_{2\text{-vsi}}$
	$c_T = 0$	$V_{0\text{-vsi}}$	$V_{7\text{-vsi}}$	$V_{0\text{-vsi}}$	$V_{7\text{-vsi}}$	V_{0_vsi}	$V_{7\text{-vsi}}$
	$c_T = 1$	$V_{5\text{-vsi}}$	$V_{6\text{-vsi}}$	$V_{1\text{-vsi}}$	$V_{2\text{-vsi}}$	$V_{3\text{-vsi}}$	$V_{4\text{-vsi}}$

2.3 DTC Principles Using Matrix Converter

According to [4], the basic DTC principles using matrix converters can be briefly described as follows: at each sampling period, the proper switching configuration, which allows the compensation of instantaneous errors in the stator flux magnitude and torque, is selected under the constraint of unity input power factor. This last requirement of the input side of the matrix converter is intrinsically satisfied if the average value of sin (ψ_i) is maintained close to zero, where ψ_i is the displacement angle between the input line voltage and input line current. The hysteresis comparator shown in figure 5c directly controls this variable and the average value of sin (ψ_i) is obtained by applying a low-pass filter to its instantaneous value. The average value of sin (ψ_i) is controlled close to zero because the input power factor is aimed close to unity.

As a facultative example, after calculation at the first time of each sampling period and considering the stator flux vector lying in sector 1, the input voltage vector lying in sector 2, the output of the torque hysteresis comparator, the flux hysteresis comparator and the hysteresis comparator of the average value of sin (ψi) are respectively c_T = +1, c_φ = 0 and c_ψ= +1. As shown in Figure 6, first with c_T = +1, c_φ = 0 and the stator flux in sector 1, the suitable voltage vector $V_{6\text{-vsi}}$ is the VSI output voltage vector by the DTC algorithm in a given switching period from Table 2. Then, with the chosen VSI voltage vector $V_{6\text{-vsi}}$, c_ψ= +1 and the input voltage vector in sector 2, the opportune matrix converter voltage vector is finally selected as $V_{\text{-5MC}}$ from Table 3.

The schematic of the DTC method using the matrix converter fed induction motor is represented in Figure 6. The reference values of the torque and the stator flux are

compared with the estimated values and coordinate with the average value of the sin (ψ_i) hysteresis comparator. In the lower part of the block diagram, the estimators of the electromagnetic torque, stator flux and the average value of sin (ψ_i) are represented. These estimators require the knowledge of input and output of voltages and currents for the matrix converter. However, only the input voltages and the output currents of the matrix converter module are measured by sensors, while other quantities such as the input voltages of the induction motor and the input currents of the matrix converter module are calculated from the previous switching states, the input voltages and the output currents of the matrix converter module.

Table 3 DTC Switching Table Using MC

Sector of $\vec{v}_i$	1		2		3		4		5		6	
c_ψ	+1	-1	+1	-1	+1	-1	+1	-1	+1	-1	+1	-1
$V_{1\text{-vsi}}$	-3_{MC}	$+1_{MC}$	$+2_{MC}$	-3_{MC}	-1_{MC}	$+2_{MC}$	$+3_{MC}$	-1_{MC}	-2_{MC}	$+3_{MC}$	$+1_{MC}$	-2_{MC}
$V_{2\text{-vsi}}$	$+9_{MC}$	-7_{MC}	-8_{MC}	$+9_{MC}$	$+7_{MC}$	-8_{MC}	-9_{MC}	$+7_{MC}$	$+8_{MC}$	-9_{MC}	-7_{MC}	$+8_{MC}$
$V_{3\text{-vsi}}$	-6_{MC}	$+4_{MC}$	$+5_{MC}$	-6_{MC}	-4_{MC}	$+5_{MC}$	$+6_{MC}$	-4_{MC}	-5_{MC}	$+6_{MC}$	$+4_{MC}$	-5_{MC}
$V_{4\text{-vsi}}$	$+3_{MC}$	-1_{MC}	-2_{MC}	$+3_{MC}$	$+1_{MC}$	-2_{MC}	-3_{MC}	$+1_{MC}$	$+2_{MC}$	-3_{MC}	-1_{MC}	$+2_{MC}$
$V_{5\text{-vsi}}$	-9_{MC}	$+7_{MC}$	$+8_{MC}$	-9_{MC}	-7_{MC}	$+8_{MC}$	$+9_{MC}$	-7_{MC}	-8_{MC}	$+9_{MC}$	$+7_{MC}$	-8_{MC}
$V_{6\text{-vsi}}$	$+6_{MC}$	-4_{MC}	-5_{MC}	$+6_{MC}$	$+4_{MC}$	-5_{MC}	-6_{MC}	$+4_{MC}$	$+5_{MC}$	-6_{MC}	-4_{MC}	$+5_{MC}$

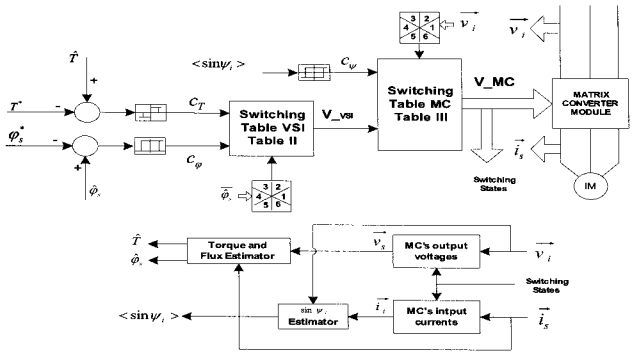

Fig. 6 Block diagram of the DTC with MC

3. Hardware Design for MC System

3.1 MC Control Board

The input voltages and output currents are measured by a 12-bit A/D converter (AD7891). The calculation of the DTC method is executed on a floating-point 32-bit DSP TMS320C32 by Texas Instrument, running at 60MHz. The DSP board includes the CAN (Control Area Network) function which is connected to a PC through a CAN card to monitor the entire system. The sampling period is 200μs, corresponding to a switching frequency of 5 kHz.

The control of the commutation process is performed by a high-CMOS (electrically erasable) programmable logic device (CPLD) board using EPM7128, manufactured by Altera, running at 40MHz. The 4-step commutation time is carried out within 2 μs. A gate driver board (TC4420) with six isolated power supplies is sufficient to drive the MC power modules.

3.2 MC Power Circuit

Figure 7 shows the hardware block diagram of a matrix converter, consisting of a 3-phase power supply and a 220V/60Hz while a 5HP induction motor is coupled with an adjustable mechanical load in order to provide the load torque. Motor's parameters are as follows

Stator Resistance	(R_s)	1.45875	(Ω)
Rotor Resistance	(R_r)	0.9058333	(Ω)
Stator Inductor	(L_s)	0.1511383	(H)
Rotor Inductor	(L_r)	0.1638935	(H)
Mutual Inductor	(L_m)	0.1483087	(H)
Number of Poles		4	

A low pass filter including a 0.5mH inductor and 20μF delta-connected capacitors, corresponding to a cut-off frequency of 1.6kHz, is connected at the power supply side.

A 7.5kW common-emitter IGBT MC module (FM35R12E3) by Eupec is used in this experiment. At the stop mode, the induction motor currents have no closing path and can cause over-voltage across the IGBT switches. The most common solution for this problem is to add 2 3-phase full diode bridges between the input and output sides, and then the energy can be stored in the small capacitor of the clamp with the acceptable over-voltage.

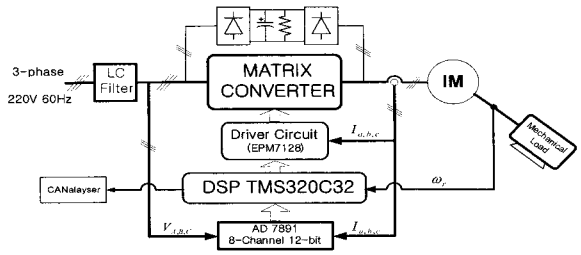

Fig. 7 Experimental block diagram of matrix converter

4. Experimental Results

Experiments are carried out to verify the validity of the DTC method for the matrix converter. The steady state performance of the matrix converter has been tested at low and high speeds. Figure 8, 9 and 10 show the motor currents for the different speed commands. The dynamic behavior has been tested under low speed changes in Figure 11 and 12, and under high speed changes in Figure 13.

Figure 14 shows the rotor speed transient state at 500 rpm as the load torque changes from 1N.m to 1.5N.m. Figure 15 shows the electromagnetic torque at the low speed of 100 rpm as the load torque command is abruptly changed. In these experimental results, the stator current waveforms are almost sinusoidal.

Furthermore, Figure 16 shows the experimental results of the motor speed at both forward and reverse directions as the speed reference changes between 200 rpm and -200rpm.

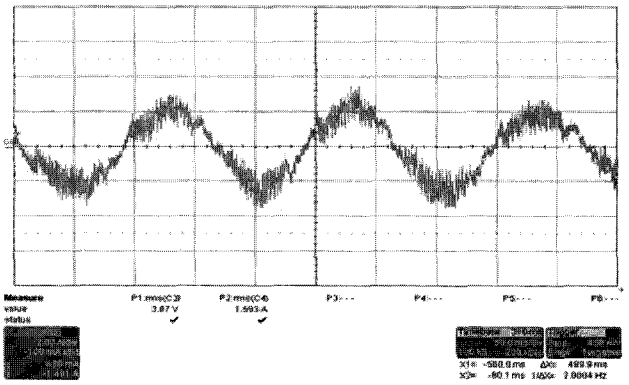

Fig. 8 Stator current at 100 rpm with 1N.m load torque

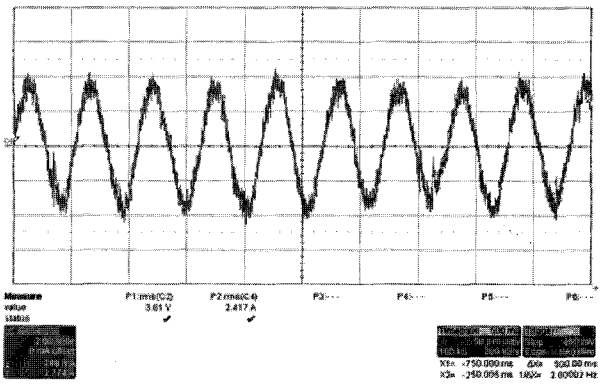

Fig. 9 Stator current at 500 rpm with 1.5 N.m load torque

Finally, Figure 17 shows the unity input power factor at the power supply side, and the harmonic spectrum analysis of the input current shows the current harmonic components, which are filtered below the cut-off frequency, 1.6kHz. However, the input current still contains many high harmonics due to the hardware limitation; the sampling frequency must be much higher to achieve an efficient implementation of DTC technique.

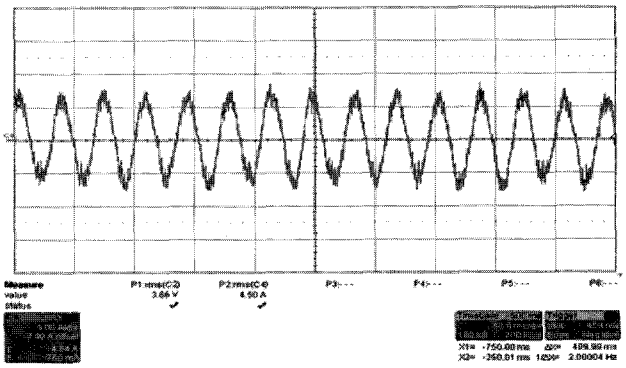

Fig. 10 Stator current at 1000 rpm with 1.5 N.m load torque

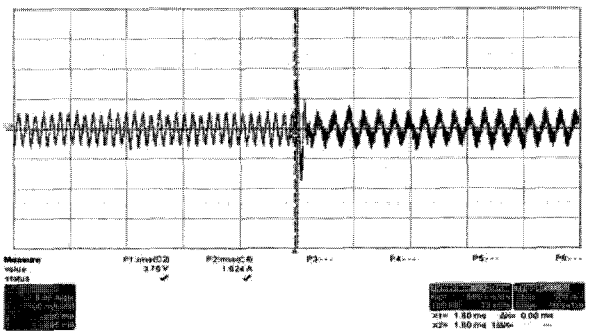

Fig. 11 Stator current with the speed change from 400rpm to 200rpm with 1 Nm

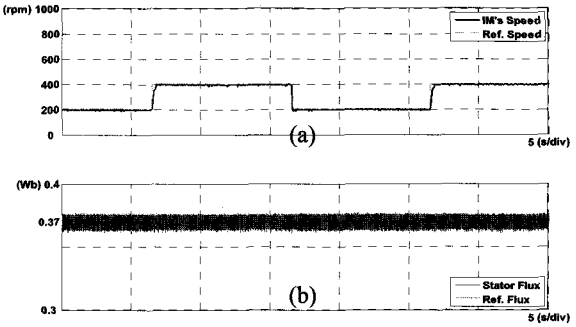

Fig. 12 (a) Rotor speed (b) Stator flux magnitude with the speed command between 200rpm and 400rpm with 1Nm

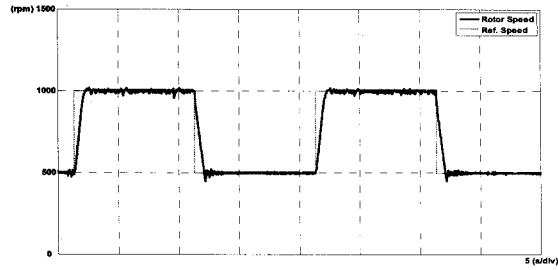

Fig. 13 Rotor speed as the reference speed change from 500 rpm to 1000 rpm with 1 Nm

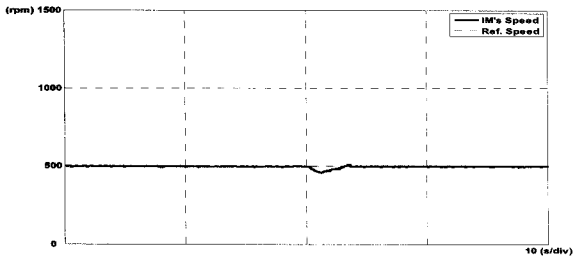

Fig. 14 Rotor speed at 500 rpm when the load torque changes from 1Nm to 1.5Nm

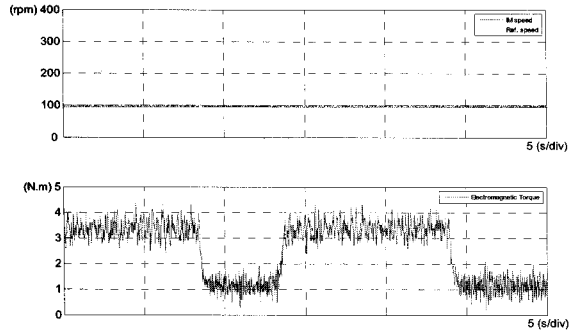

Fig. 15 Electromagnetic torque with the load torque command between 3.5 Nm and 1 Nm

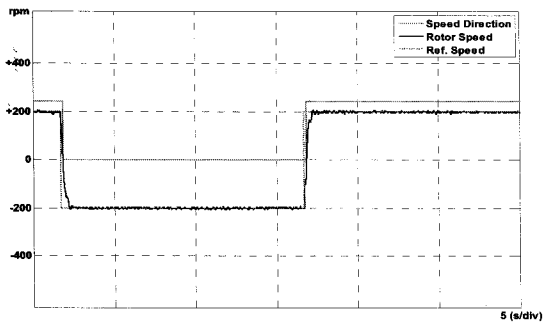

Fig. 16 Rotor speed in the forward and reverse directions

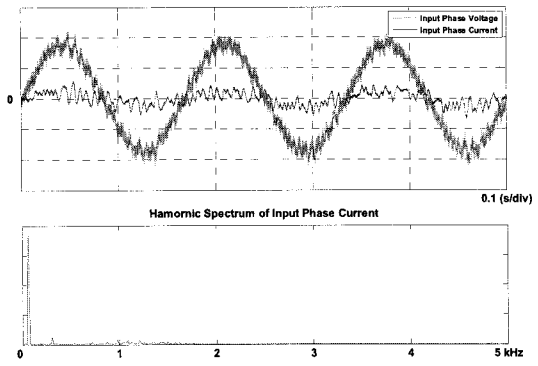

Fig. 17 Input line to neutral voltage (100V/div)and input line current (10A/div) waveforms with 3.5 Nm torque command

5. Conclusions

This paper deals with the experimental implementation with the DTC method using the matrix converter fed induction motor. This inherits the advantages of the DTC method and the advantages of the matrix converter characteristics. The experimental environment is explained in detail. The steady and transient experimental results are shown to validate the stability and the robustness of the DTC method in the practical applications. With an improved hardware design, the DTC method using the matrix converter may become the most appropriate solution to build a compact drive fed induction motor.

Acknowledgment

The authors would like to thank Ulsan Metropolitan city, the MOCIE and the MOE of the Korean Government which partly supported this research through the Network-based Automation Research Center (NARC) and the Post BK 21 Program at University of Ulsan.

References

[1] E. Watanabe, S. Ishii, E. Yamamoto, H. Hara, Jun-Koo Kang & A.M. Hava, "High performance motor drive using matrix converter", Advances in Induction Motor Control (Ref. No. 2000/072), IEE Seminar, May 2000.

[2] T. Matsuo, S. Bernet, R.S. Colby & T.A. Lipo, "Application of the matrix converter to induction motor drives", Thirty-First IAS Annual Meeting Conference Record, Vol.1, pp.60 – 67, Oct. 1996.

[3] Romeo Ortega, Nikita Barabanov & Gerardo Escobar Valderrama, "Direct Torque Control of Induction Motors: Stability Analysis and Performance Improvement", IEEE transactions on automatic control, Vol. 46, No. 8, August 2001.

[4] D. Casadei, G. Serra & A. Tani, "The use of matrix converters in direct torque control of induction machines", Conference Proceedings of IECON '98, Vol. 2, pp.744 – 749, Sept. 1998.

[5] Hong-Hee Lee & Minh-Hoang Nguyen, "Matrix converter fed induction motor using a new modified direct torque control method", Conference Proceedings of IECON 2004, Vol. 3, pp.2301 – 2306, Nov. 2004.

[6] Guo qiangang, Li yaohua, Meng Yanjing & Liu Weiguo, "Modeling and simulation study on matrix converter fed induction motor drive system implemented by direct torque control", Proceedings of the Eighth International Conference on Electrical Machines and Systems, Vol. 2, pp.1069 – 1074, Sept. 2005.

Hong-Hee Lee received his B.S., M.S., and Ph.D. degrees from Seoul National University, Seoul, Korea. Currently, he is a Professor at the School of Electric-Electronic Information System Engineering, University of Ulsan, Ulsan, Korea. He is also Director of the Network-based Automation Research Center (NARC), which is sponsored by the Ministry of Commerce, Industry and Energy (MOCIE). His research interests are power electronics, network-based motor control, and control network. He is a member of IEEE, KIEE, KIPE, and ICROS.

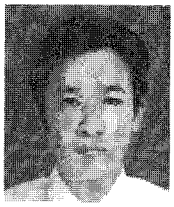

Hoang M. Nguyen was born in Nha Trang, Vietnam, in 1979. He received his B.S. degree in Electrical Engineering from the University of Technology, HoChiMinh, Vietnam in 2002 and his M.S. degree from the University of Ulsan, Korea in 2005. He is currently a Ph.D. student at the University of Ulsan, Ulsan, Korea. He is engaged in research on motor control, especially matrix converters and industrial networks.

Tae-Won Chun was born in Korea in 1959. He received his B.S. degree in Electrical Engineering from Pusan National University in 1981, and received his M.S. and Ph.D. degrees in Electrical Engineering from Seoul National University in 1983 and 1987, respectively. Since 1986, he has been a member of the faculty of the Department of Electrical Engineering, Ulsan University, where he is currently a Full Professor. His current research interests are control of electrical machines, power converter circuits, and industrial applications.